

SIGNIFICANCE OF VISCOUS DISSIPATION AND POROSITY EFFECTS IN A HEATED SUPERHYDROPHOBIC MICROCHANNEL

G. Ojemer¹ and I. O. Onwubuya²

¹Department of Mathematics, College of Sciences, Federal University of Agriculture, P. M. B. 28, Zuru, Kebbi State, Nigeria.

²Department of Mathematics, Faculty of Sciences, Air Force Institute of Technology, P. M. B. 2104, Kaduna State, Nigeria.

*corresponding: godwinojemer@gmail.com

Article history:

Received Date:

15 February
2023

Revised Date:

10 October 2023

Accepted Date:

20 October 2023

Keywords:

Super-
Hydrophobic
Slip,
Temperature

Abstract— The theoretical treatment of heat enhancement flow for an electrically conducting and viscous dissipative fluid traveling vertically through a thermodynamic system where the parallel plates are constantly heated in a slit microchannel filled with porous material is investigated in this work. One surface had superhydrophobic slip and a temperature jump, whereas the other did not. The perturbation technique (semi-analytical method) was employed to solve the nonlinear and coupled leading equations. It is concluded from this analysis that the fluid temperature and velocity were found to increase as the

This is an open-access journal that the content is freely available without charge to the user or corresponding institution licensed under a Creative Commons Attribution-NonCommercial-NoDerivatives 4.0 International (CC BY-NC-ND 4.0).

Jump, Viscous Dissipation, Porous Medium, Slit Micro- Channel	viscous dissipation term increased. Similarly, the function of Darcy's porous number is to significantly strengthen the fluid velocity, and these effects are stronger at the heated super-hydrophobic surface, whereas the mounting level of the magnetic field is seen to drastically weaken the fluid motion in the microchannel. Setting the Brickman number, Br , to zero and the porous parameter, K , to 1000, so that the term becomes insignificant, Jha and Gwandu (2017)'s work is retrieved, verifying the accuracy of the current analysis. Further, the outcomes of this research can have possible applications in the lubrication industry and biomedical sciences and have proved very useful to designers in increasing the performance of mechanical systems when viscous dissipation is involved, as well as heat transfer in micro-channels, as it is in combustion.
---------------------------------------------------------------------------	-----------------------------------------------------------------------------------------------------------------------------------------------------------------------------------------------------------------------------------------------------------------------------------------------------------------------------------------------------------------------------------------------------------------------------------------------------------------------------------------------------------------------------------------------------------------------------------------------------------------------------------------------------------------------------------------------------------------------------------------------------------------------------------------------------------------------------------------------------------------------------------------------

I. Introduction

The tremendous growth of technology in response to people's desires for smaller machines and lighter devices directs the scientific community, engineers, and innovators' attention to exploration, simulation, and theoretical investigations in mini-technology, then micro-

technology, and finally nano-technology. This is what prompted fluid mechanics experts to go from researching flows in macro-channels to researching flows in mini-channels, micro-channels, and nano-channels. Micro-channel fluid and thermal transport flows have grown tremendously in recent times as a result of their

wide spectrum of interesting applications in material processing activities and fabrication; micro energy pipes; space technology; micro-channel internal heat generation; micro-jet boundary layer cooling; large power density transistors in high-performance computing; and other devices. Since most of these designs involve internal micro-channel flows, comprehending the flow characteristics has become extremely crucial for proper and appropriate simulation projections and conceptualization [1-2]. Numerous studies have been published on the role of the flow regime on micro-geometry in a number of physical situations. In light of the foregoing, Ojemeru and Hamza [3] recently presented a theoretical investigation of Arrhenius-kinetically driven heat source and sink fluid in a microchannel using the homotopy perturbation technique. Jha and Malgwi [4] analyzed the effects of Hall current and ion-slip on hydro-magnetic heat transfer flow in a vertical micro-channel with an

applied magnetic field. Jha and Aina [5] comprehensively addressed natural convection driven hydro-magnetically in a vertical micro-channel made of two electrically non-conducting infinite vertical parallel plates. In another work, Jha et al. [6] deliberated on the consequences of Hall currents on hydro-magnetic natural convection in a vertical micro-channel. References that shed more light on this field of interest include [7 - 11], to name a few.

Magneto - hydrodynamics (MHD) research has evolved in prominence in recent decades owing to the concept's benefits in a range of MHD applications, namely MHD generators, optical grafting, metal casting, crystal growth, and magneto-hydrodynamic injectors. Several nuclear power facilities already use chemical energy technology, which incorporates the use of MHD pumps to move electrically conductive fluids. In addition to these applications, when the fluid is electrically conducting, an applied magnetic field can considerably increase free convection flow [12].

Various studies have been conducted on hydro-magnetic convective flow in a spectrum of environmental situations. To this end, Hamza et al. [13] evaluated the convectively heated, MHD-free flow of a chemically reacting fluid in a vertical channel imagined with porous media. The steady-state component was determined using the homotopy perturbation method, while the unsteady-state case was analyzed using a numerical technique. In a different paper, Hamza et al. [14] discussed the implications of MHD on the natural convective slip flow of an exothermic fluid due to Newtonian heating. Taid and Ahmed [15] used the perturbation approach to probe the impacts of the Soret effect, heat dissipation, and chemical reaction on steady two-dimensional hydro-magnetic natural convection across an inclined porous plate coated with porous media. Osman et al. [16] searched the function of MHD on free convection over an infinitely inclined plate using the Laplace transformation

technique. Siva et al. [17] presented a precise response to the MHD action on a heat enhancement study of electroosmotic flow in a rotating microfluidic channel. Heat and mass transportation were probed for viscoelastic MHD boundary layer flow past a vertical flat plate by Choudhary [18]. The actions of an inclined magnetic field on the time-dependent natural convection flow of a dusty viscous fluid within two infinite flat plates packed with a porous material were examined by Sandeep and Sugunamma [19]. When Joseph et al. [20] discussed unsteady MHD Poiseuille flow across two infinitely parallel porous plates in an inclined magnetic field, they also considered the impacts of heat and mass transport. They discovered that as the Hartman number Ha grows, the velocity drops. Velocity rises due to the thermal Grashof number Gr and the solutal Grashof number Gc influences. A boost in the Prandtl number, Pr , leads to a decay in the fluid temperature. As the chemical parameters Kc and Sc rise, so does the

concentration of a species. Geethan et al. [21] scrutinized the joint consequences of thermal radiation, chemical reaction, and Soret on hydro-magnetic free convection slip flow along an inclined plate with a constant temperature affected by the heat source. A computational analysis of the Hall current and thermal radiation effects of MHD natural convective mass and energy transfer radiating fluid flow in the Soret effect and heat generation was accounted for by Sivaiah and Reddy [22]. Scientists, technologists, and engineers are paying much attention to the evaluation of the result of the new combination using hydro-magnetic natural convection flow in a superhydrophobic (SHO) microchannel. Oil and gas companies, semiconductor manufacturing facilities, and companies that assemble small equipment on SHO surfaces have the ability to reduce drag in a flow because of the enormous slip obtained from liquid/solid interfaces, making it a particularly relevant parameter to gauge the extent of drag

reduction depending on the slip length. In view of these considerations, a theoretical investigation of MHD natural convection in a vertical slit micro-channel having a superhydrophobic slip effect and temperature jump was conducted by Jha and Gwandu [1]. Their research showed that the greatest upward velocity obtained by heating the superhydrophobic wall is less than that attained by heating the no-slip surface whenever there is a temperature leap and no superhydrophobic slip, or both. The maximum velocities are equivalent when neither is present. Later, Jha and Gwandu [23] investigated the free convection flow of an electrically conducting fluid in a vertical slit microchannel affected by superhydrophobic slip and temperature jump effects using the non-linear Boussinesq approximation methods. Raising the temperature jump coefficient, according to the computational results, contributes to a decrease in temperature when the superhydrophobic surface is heated

and increases the temperature when the no-slip surface is heated. Jha and Gwandu [24] built on their previous work, Jha and Gwandu [1] by proposing an analytical investigation of free convection airflow across porous plates heated alternately, one channel with no slip and the other super-hydrophobic. Ramanuja et al. [25] explored free convection flow in an isothermally heated channel with super-hydrophobic slip on one surface and a temperature rise but no slip on the opposite side. Hatte and Pitchumani [26] used a fractional rough surface characterization to thoroughly and explicitly describe the impact of heat transfer flow inside a cylinder with non-wetting surfaces. The approach examines the dynamic stability of the air-fluid interaction in the asperities of air-infused super-hydrophobic surfaces. Their findings show that, contrary to prevalent belief, super-hydrophobicity, defined by the largest contact angles, does not always result in peak convective heat transfer behavior and that, under specific fluid flow

conditions, hydrophobic surfaces can provide excellent thermal performance.

The actions of viscous dissipation and Darcy permeability on micro-channels with super-hydrophobic (SHO) surfaces have not been examined in any of the above-mentioned literature, which prompted the interest in this research. Thus, motivated by the above knowledge gap, the focus of this paper is to theoretically investigate the impact of MHD-free convection flow of viscous dissipative fluid in a vertical parallel plate that is constantly heated in a slit microchannel having a super-hydrophobic surface filled with porous media. To the best of the authors' knowledge, this research has not been documented in any earlier literature, resulting in the study's novelty. A semi-analytical approach (the perturbation method) was employed to solve the dimensionless nonlinear and coupled governing equations. The behaviors of controlling parameters on temperature, velocity, heat transfer rate, and shear stress were computed and

discussed with the help of illustrative graphs. Internal heating is a type of mechanical energy dissipation that is spurred on by viscous forces in molecular fluid-particle exchanges. This particular kind of mechanical energy dissipation has a major effect on the fluid's hydrodynamic and thermodynamic behavior, and its attributes have a wide range of applications in the lubrication, food processing, and food preservation industries, as well as in the cooling of electrical appliances, exploration for petroleum products, and other industries.

II. Mathematical Formulation of the Problem

Imagine an electrically conducting fluid traveling gradually upward within a vertical parallel plate microchannel heated alternatively by wall constant temperature. Due to a particular micro-engineering treatment, one of the surfaces is exceedingly difficult to wet (super-hydrophobic). The

opposite wall (no-slip surface) was unaltered. As shown in Figure 1, the super-hydrophobic wall is kept at $y_0 = 0$, while the no-slip surface is kept at $y_0 = L$. Since the ultimate focus is on the superhydrophilicity of a surface rather than the flow behavior, various temperature jump and slip conditions were applied to the plates. The governing equations for the current problem, employing the Boussinesq buoyancy approximation with boundary conditions, assuming that the fluid is viscous and has permeability effects, can be written in dimensionless form, following Jha and Gwandu [1] and Ajibade and Umar [26]:

$$\frac{d^2U}{dy^2} + \theta - (M^2 + \frac{1}{K})U = 0 \quad (1)$$

$$\frac{d^2\theta}{dy^2} + Br \left(\frac{du}{dy}\right)^2 = 0 \quad (2)$$

The boundary conditions in dimensionless forms are:

$$\theta(0) = 1 + \gamma \frac{d\theta}{dy}, u(0) = \lambda \frac{du}{dy} \quad (3)$$
$$\theta(1) = 0, u(1) = 0$$

where:

M = magnetic field intensity
 K = permeability of the porous medium
 $Br = EcPr$ is the Brinkman number
 γ = temperature jump coefficient
 λ = velocity slip condition

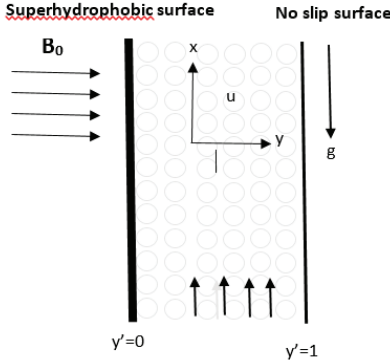


Figure 1: Schematic of the fluid flow in a slit microchannel with a porous configuration

The dimensional quantities used in deriving Equations (1) – (3) are as follows:

$$y = \frac{y'}{h}, u = \frac{u'}{U}, T = \frac{T' - T_0}{T_w - T_0},$$

$$(Y, \gamma, \Gamma) = \frac{Y', \gamma', \Gamma'}{h},$$

$$M^2 = \frac{\sigma \beta_0^2 h^2}{\rho v}, Br = \frac{hH}{k}, K = \frac{k}{h^2}$$

All the constants used are declared in the nomenclature.

III. Method of Solution

The velocity and energy equations can be reduced to a set of ordinary differential equations, which are solved semi-analytically by the perturbation method. We assume,

$$\left. \begin{aligned} \theta &= \theta_o + Br_r \theta_1 \\ U &= U_o + Br_r U_1 \end{aligned} \right\} \quad (4)$$

Substituting Equation (4) into Equation (1) – (3) and taking the coefficient of Br^o and Br_r , we have

$$Br^o: \frac{d^2 U_o}{dy^2} + \theta_o - (M^2 + \frac{1}{K})U_o = 0 \quad (5)$$

$$Br_r: \frac{d^2 U_1}{dy^2} + \theta_1 - (M^2 + \frac{1}{K})U_o = 0 \quad (6)$$

$$Br^o: \frac{d^2 \theta_o}{dy^2} = 0 \quad (7)$$

$$Br_r: \frac{d^2 \theta_1}{dy^2} + (\frac{dU_o}{dy})^2 = 0 \quad (8)$$

The boundary conditions at both walls now becomes:

$$\left. \begin{aligned} Br_r: \theta_1 &= \gamma \frac{d\theta_1}{dy} \\ U_1 &= \lambda \frac{dU_1}{dy} \end{aligned} \right\} \text{at } y = 0 \quad (9)$$

$$\left. \begin{aligned} U_o &= \lambda \frac{dU_o}{dy} \\ U_1 &= \lambda \frac{dU_1}{dy} \\ U_o &= 0 \\ U_1 &= 0 \end{aligned} \right\} \text{at } y = 1 \quad (10)$$

$$\left. \begin{aligned} \theta_0 &= 1 + \gamma \frac{d\theta_0}{dy} \\ \theta_1 &= \gamma \frac{d\theta_1}{dy} \\ \theta_0 &= 0 \\ \theta_1 &= 0 \end{aligned} \right\} \begin{array}{l} \text{at } y = 0 \\ \text{at } y = 1 \end{array} \quad (11)$$

Solution for temperature distribution is derived as follows:

$$\theta_0 = C_1 y + C_2 \quad (12)$$

$$\theta_1 = -\frac{b_1}{4m^2} e^{2my} - \frac{b_2}{m^2} e^{my} - \frac{b_3}{m^2} e^{-my} - \frac{b_4}{4m^2} e^{-2my} - b_5 \frac{y^2}{2} + C_7 y + C_8 \quad (13)$$

Solution for velocity distribution is obtained as follows:

$$U_0 = C_3 e^{my} + C_4 e^{-my} + C_5 y + C_6 \quad (14)$$

$$U_1 = D_1 e^{my} + D_2 e^{-my} + D_3 e^{2my} + D_4 y e^{my} + D_5 y e^{-my} + D_6 e^{-2my} + D_7 y^2 + D_8 y + D_9 \quad (15)$$

$$\text{Since } \theta = \theta_0 + B_r \theta_1 \quad (16)$$

Then,

$$\theta = C_1 y + C_2 + B_r \left[-\frac{b_1}{4m^2} e^{2my} - \frac{b_2}{m^2} e^{my} - \frac{b_3}{m^2} e^{-my} - \frac{b_4}{4m^2} e^{-2my} - b_5 \frac{y^2}{2} + C_7 y + C_8 \right] \quad (17)$$

$$\text{also, since } U = U_0 + B_r U_1 \quad (18)$$

Then,

$$U = C_3 e^{my} + C_4 e^{-my} + C_5 y + C_6 + B_r [D_1 e^{my} + D_2 e^{-my} + D_3 e^{2my} + D_4 y e^{my} + D_5 y e^{-my} + D_6 e^{-2my} + D_7 y^2 + D_8 y + D_9] \quad (19)$$

The heat transfer rate and frictional force at both plates are derived as follows:

$$\frac{d\theta}{dy} \Big|_{y=0} = C_1 + B_r \left[-\frac{b_1}{2m} - \frac{b_2}{m} + \frac{b_3}{m} + \frac{b_4}{2m} + C_7 \right] \quad (20)$$

$$\frac{d\theta}{dy} \Big|_{y=1} = C_1 + B_r \left[-\frac{b_1}{2m} e^{2m} - \frac{b_2}{m} e^m + \frac{b_3}{m} e^{-m} + \frac{b_4}{2m} e^{-2m} - b_5 + C_7 \right] \quad (21)$$

$$\frac{dU}{dy} \Big|_{y=0} = C_3 m - C_4 m + C_5 + B_r [D_1 m - D_2 m + 2D_3 m + D_4 + D_5 - 2D_6 m + D_8] \quad (22)$$

$$\frac{dU}{dy} \Big|_{y=1} = C_3 m e^m - C_4 m e^{-m} + C_5 + B_r [D_1 m e^m - D_2 m e^{-m} + 2D_3 m e^{2m} + D_4 m e^m + D_4 e^m + D_5 m e^{-m} + D_5 e^{-m} - 2D_6 m e^{-2m} + 2D_7 + D_8] \quad (23)$$

All the constants are defined in the appendix section.

IV. Results and Discussions

The current study looked into the combined influences of MHD and viscous dissipation on the steady free flow of an incompressible electrically conducting fluid traveling vertically inside an isothermally heated parallel plate microchannel saturated with porous material, with one surface having super-hydrophobic slip and a temperature jump and the

other having no slip. The perturbation series approach (semi-analytical method) is used to evaluate the steady-state governing equations. Several graphs were drawn to showcase the influences of various settings on the flow configuration and energy profile.

The default values chosen for this research are ($\lambda = \gamma = 1, M = 0.5, Br = 0.001, K = 0.1$), except otherwise stated, as they relate to real-life situations.

Figures 2 and 3 show the impact of the Brinkman number (Br) on dimensionless thermal and momentum distributions for fixed values of ($\lambda = \gamma = 1$). It is

obvious from these figures that the thermal and mechanical properties of the fluid increase dramatically as the local Brinkman number (Br) increases. Higher Brinkman values indicate stronger convective heating at the lower channel surface, resulting in a better temperature and velocity at the lower plate. Makinde and Aziz [27] opined that uplifting the local Brinkman numbers makes the convective heating at the lower channel wall stronger. This leads to higher surface temperatures and lets the thermal effect go deeper into the still fluid.

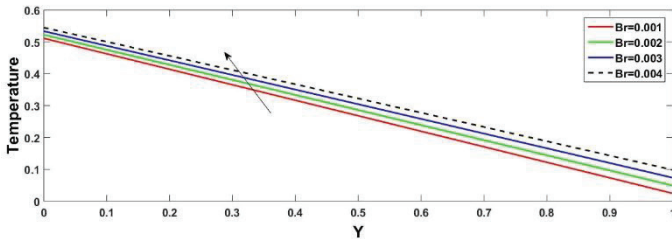


Figure 2: Deviation of temperature for Br for constant values of ($\lambda = \gamma = 1, M = 0.5, K = 0.1$)

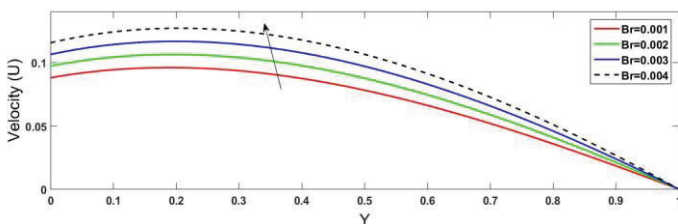


Figure 3: Deviation of velocity for Br for constant values of ($\lambda = \gamma = 1, M = 0.5, K = 0.1$)

Figure 4 depicts the action of the Darcy porosity parameter on the velocity gradient. It is apparent from this figure that the fluid velocity accelerates as the porosity parameter is increased. We observe that, with the growth in permeability of the porous medium, the drag force

weakens; because of this, the velocity gradient of the fluid improves. Moreover, this makes sense because when a lot of fluid is moved, more viscous energy is produced. This causes the fluid boundary wall and thickness to grow, which speeds up the movement of the fluid.

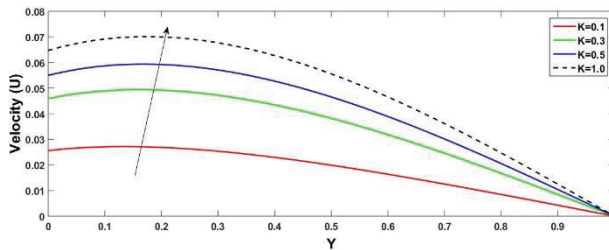


Figure 4: Deviation of velocity for K for constant values of ($\lambda = \gamma = 1, M = 0.5$)

With the help of Figure 5, we comprehend how velocity distribution behaves against displacement y , and the outcome is consistent with what has been discovered in previously published results by other authors, such as the works of Jha and Gwandu [1][23]. This demonstrates that as particles

move out from the superhydrophobic side, their velocity increases for a short time before petering out as they approach the center. However, if both surfaces are not superhydrophobic, the velocity does not rise significantly and does not fall until near the channel's center.

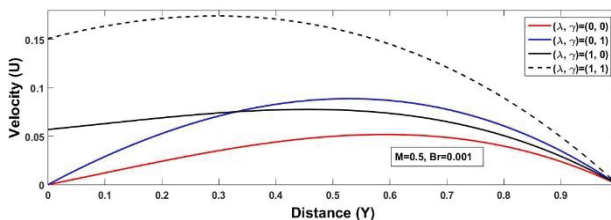


Figure 5: Deviation of velocity for the displacement y for constant values of ($M = 0.5, Br = 0.001, K = 0.1$)

Figure 6 shows the function of MHD on the velocity gradient. The pattern demonstrates a decrease in the fluid flow (particularly the peak velocity) as the magnetic field intensity increases (when both λ and γ are equal to unity). This is attributable to the Lorentz force,

which appears when a magnetic field imposes itself on an electrically conducting fluid and a drag force is created. Due to this force, fluid movement dwindles near the plate; all other forces, including the Lorentz force, peter out as a result when the fluid comes to rest.

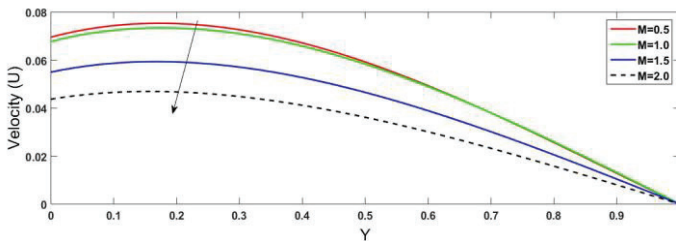


Figure 6: Deviation of velocity for MHD for constant values of ($\lambda = \gamma = 1$, $Br = 0.001, K = 0.1$)

Figures 7 and 8 show the implication of the Brinkman number (Br) on the rate of heat transfer coefficient and wall shear stress. Heat transfer rate increases with growing values of the Brinkman number in both walls. The effect of large Br is seen to strengthen the frictional force (at $y = 0$), as shown in Figure 8(a), whereas a reverse trend is obtained (at $y = 1$), as depicted in Figure 8(b).

Figure 9 displays the action of a magnetic field on skin friction.

It is clear that MHD has the same effect on shear stress on both plates, but this impact is stronger on the plate where $y = 0$.

The response of varying Darcy porous numbers to frictional force at both plates is plotted in Figure 10. It is noticeable that raising the level of porous parameter encourages skin friction at the plate ($y = 0$), as elucidated in Figure 10(a), whereas in Figure 10(b), a counter attribute happens at the plate ($y = 1$).

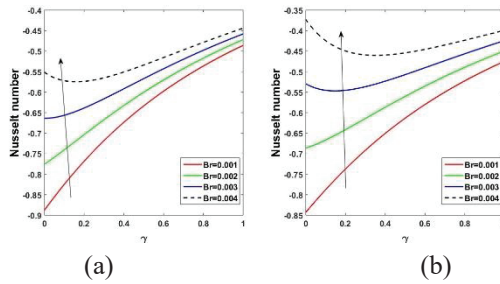


Figure 7: Variation for Nusselt number for Br at (a) $y=0$ and (b) $y=1$ for constant values of ($\lambda = \gamma = 1, M = 0.5, K = 0.1$)

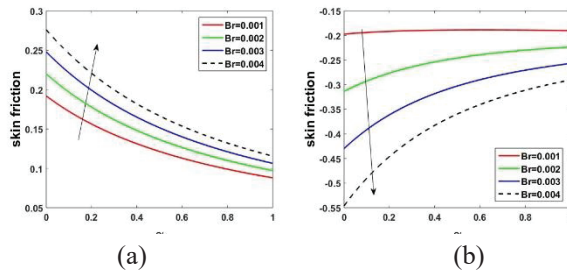


Figure 8: Variation for skin friction for Br at (a) $y=0$ and (b) $y=1$ for constant values of ($\lambda = \gamma = 1, M = 0.5, K = 0.1$)

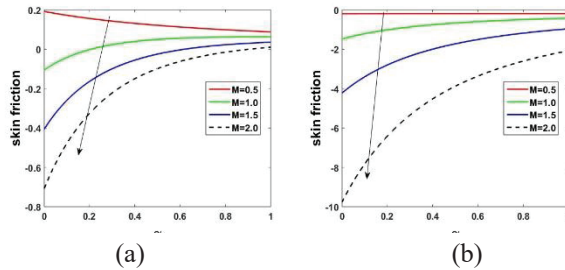


Figure 9: Variation for skin friction for M at (a) $y=0$ and (b) $y=1$ for constant values of ($\lambda = \gamma = 1, Br = 0.001, K = 0.1$)

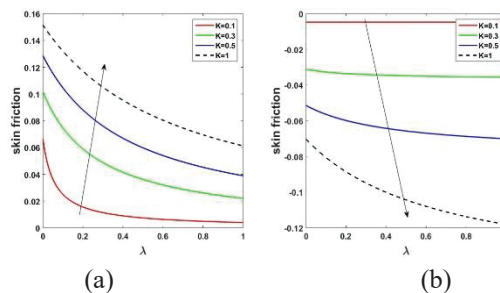


Figure 10: Variation for skin friction for K at (a) $y=0$ and (b) $y=1$ for constant values of ($\lambda = \gamma = 1, M = 0.5, Br = 0.001$)

V. Verification

The work of Jha and Gwandu [1] is retrieved by setting $Br = 0$ and $K = 1000$, thereby confirming an excellent agreement between this present

research and their work. Table 1 describes the numerical computations of the comparison between the work of Jha and Gwandu [1] and the current investigation.

Table 1: Computations of comparison between the work of Jha and Gwandu [1] with the current analysis for temperature and velocity distributions for $\lambda = \gamma = 1$, $M = 0.5$ when $Br = 0$, and $K = 1000$

Y	Jha and Gwandu [1]		Present work	
	θ (Y)	U (Y)	θ (Y)	U (Y)
0.1	0.4500	0.0843	0.4500	0.0843
0.2	0.4000	0.0856	0.4000	0.0856
0.3	0.3500	0.0831	0.3500	0.0831
0.4	0.3000	0.0772	0.3000	0.0772
0.5	0.2500	0.0686	0.2500	0.0686

VI. Conclusions

The current study looked at the consequences of Darcy porous number and viscous dissipation on the steady flow of a viscous, electrically conducting fluid traveling vertically across an isothermally heated parallel plate micro-channel embedded with porous medium, with one surface exhibiting super-hydrophobic slip and a temperature jump and the other not. A semi-analytical method (perturbation series approach) was employed to generate the steady-state solutions for temperature, velocity, rate of

heat transfers, and shear stress. The influence of pertinent parameters dictating the flow configuration is discussed in detail using various plots. Viscous dissipation and Darcy porous effects are vital in most lubrication industries. This study can therefore find relevance in science, engineering, and industrial technologies such as cooling of electrical appliances, geothermal energy, porous solids drying, thermal insulation, gas drainage, plasma physics, gas turbines, fossil fuel combustion, and food

processing industries, to mention a few.

The following is an overview of the significant findings from this study:

- (i) The maximum velocity attained by heating the super-hydrophobic surface is smaller than that recorded by heating the no-slip surface when there is a temperature jump and no super-hydrophobic slip or both. The opposite is true if there is a super-hydrophobic slide but no temperature surge. When neither exists, the maximum velocities are equal.
- (ii) As the Brinkman number parameter goes up, the velocity of the fluid and the heat gradient grow noticeably, but the local skin friction goes down at $y = 1$ and up at $y = 0$.
- (iii) Upon increasing the Darcy permeability parameter, drag forces diminish; hence, the fluid mobility in the micro-channel significantly improves. Also, the sheer stress at both micro-channel

walls exhibits comparable trends with the same consequence.

- (iv) The velocity gradient peters out upon raising the levels of the magnetic parameter due to the Lorentz forces, which manifest under the MHD effect.
- (v) By uplifting the values of Br , the heat transfer rate shows similar increasing trends at both the no-slip and the super-hydrophobic surfaces.
- (vi) In the future, this research will be expanded to consider the unsteady state (time-dependent) case, the heat-generating or absorbing effect, or a different physical geometry.

VII. Acknowledgement

The first author conceptualized the problem and provided the methodology as well as the main draft of the manuscript. The second author contributed to the analysis, validation, and editing of this work. All authors read and approved the final manuscript.

VIII. References

- [1] B. K. Jha and B. J. Gwandu, "MHD free convection flow in a vertical slit micro-channel with super-hydrophobic slip and temperature jump: Heating by constant wall temperature", *Journal of Alexandria Engineering*. vol. 57, no. 3, pp. 2541-2549, 2017.
- [2] B. K. Jha, B Aina and A. T. Ajiya, "MHD natural convection flow in a vertical parallel plate microchannel", *Ain shams Eng.J.* vol. 6, pp. 289-295 2014a.
- [3] G. Ojemeru, M. M. Hamza, "Heat transfer analysis of arrhenius-controlled free convective hydromagnetic flow with heat generation/absorption effect in a micro-channel", *Alexandria Eng. J.* vol. 61, pp. 12797-12811, 2022.
- [4] B. K. Jha and P. B. Malgwi, "Hall current and ion – slip effects on free convection flow in a vertical microchannel with induced magnetic field", *Heat Transf. Asian Res.* vol. 48, no. 8, pp. 1 – 19. 2019a.
- [5] B. K. Jha and B. Aina, "Role of induced magnetic field on MHD natural convection flow in vertical microchannel formed by two electrically non-conducting infinite vertical parallel plates", *Alexandria Eng. J.* vol. 55, no. 2, pp. 2087-2097, 2016.
- [6] B. K. Jha, P. B. Malgwi, B. Aina, "Hall effects on MHD natural convection flow in a vertical microchannel", *Alexandria Eng. J.* 2017.
<http://dx.doi.org/10.1016/j.aej.2017.01.038>
- [7] C. K. Chen and H. C Weng, "Natural convection in a vertical micro-channel", *J. Heat Transf.* vol. 127, pp. 1053-1056, 2005.
- [8] B. K. Jha and B. Aina, "Mathematical modelling and exact solution of steady fully developed mixed convection flow in a vertical micro-porous-annulus", *J. Afrika Matem-atika*, vol. 26, pp. 1199-1213, 2015.
- [9] B. Buonomo and O. Manca, "Natural Convection Flow in a Vertical Micro-Channel with Heated at Uniform Heat Flux", *Int. J. Therm.Sci.* vol. 49, pp. 1333-1344, 2012.
- [10] H. C. Weng and C. K. Chen, "Drag reduction and heat transfer enhancement over a heated wall of a vertical annular microchannel", *Int. J. Heat Mass Transf.* vol. 52, pp. 1075–1079, 2009.
- [11] B. K. Jha, B. Aina and S. B. Joseph, "Natural Convection Flow in vertical Micro-channel with Suction/Injection", *J. Proc. Mech. Eng.*, vol. 228, no. 3, pp. 171-180, 2014b.
- [12] B. K. Jha, B. Aina and S. Isa, "Fully developed MHD natural convection flow in a vertical annular micro channel: an exact solution", *J. king Saudi Univ Sci.*, vol. 27, pp. 253-259, 2015.
- [13] M. M. Hamza, S. Abdulsalam and A. S. Kamba, "Unsteady

- MHD free convection flow of an exothermic fluid in a convectively heated vertical channel filled with porous medium”, *Scientific Reports*, vol. 12, 11989, 2022.
- [14] M. M. Hamza, M. Z. Shehu and B. H. Tambuwal, “Steady state MHD free convection slip flow of an exothermic fluid in a convectively heated vertical channel”, *Saudi J Eng Technology*. DOI: 10.36348/sjet.2021.vo6i10.006 (2021).
- [15] B. K. Taid and N. B. Ahmed, “MHD free convection flow across an inclined porous plate in the presence of heat source, Soret effect and chemical reaction affected by viscous dissipation ohmic heating”, *Bio-interface Res Applied Chem*, vol. 12, no. 5, pp. 6280-6296, 2022.
- [16] Husna Izzati Osman et al. A study of MHD free convection flow past an infinite inclined plate. *J Adv Res fluid Mech Therm Sci*, vol. 92, no. 1, pp. 18-27, 2022.
- [17] T. Sova, S. Jaangili and B. Kumbhakar, “Heat transfer analysis of MHD and electroosmotic flow of non-Newtonian fluid in a rotating microfluidic channel: an exact solution”, *Appl Math Mech*, vol. 42, 1047-1062, 2021.
- [18] D. Chaudhary, “Heat and Mass Transfer for visco-elastic MHD Boundary Layer Flow Past a Vertical Plate”, *Theo Appl Mech*, vol. 33, pp. 281-309, 2012.
- [19] N. Sandeep and V. Sugunamma, “Effect of an Inclined Magnetic Field on Unsteady free Convection flow of a Dusty Viscous fluid between two Infinite flat Plates filled by a Porous medium”, *Int. J. Appl. Math Mod* vol. 1, no. 1, pp. 16-33. 2013.
- [20] K. M. Joseph, P. Ayuba, L. N. Nyitor and S.M. Muhammed, “Effect of Heat and Mass Transfer on Unsteady MHD Poiseuille flow between Two Infinite Parallel Porous plates in an Inclined Magnetic Field”, *Int. J. of Sci Eng and Appl Sci*. vol. 1, no. 5, 2015.
- [21] S. K. Geethan, R. K. Kiran, G. K. Vinod and V Varma, “Soret and Radiation Effects on MHD Free Convection Slip Flow over an Inclined Porous Plate with Heat and Mass Flux”, *Adv Sci Eng Med*, vol. 8, no. 3, pp. 1-10, 2016.
- [22] G. Sivaiah and K. J. Reddy, “Unsteady MHD heat and mass transfer flow of a radiating fluid Past an Accelerated Inclined Porous Plate with Hall Current”, *Int. Research-Granthaalayah*, vol. 5, no. 7, pp. 42-59, 2017.
- [23] B. K. Jha and B. J. Gwandu, “MHD free convection flow in a vertical slit micro-channel with superhydrophobic slip and temperature jump: non-linear Boussinesq approximation approach”, *SN Applied Sciences*, DOI: 10.1007/S42452-019-0617-Y, 2019.

- [24] B. K. Jha and B. J. Gwandu, "MHD free convection flow in a vertical porous super-hydrophobic microchannel", Proceedings of the inst. Of mech engineers; part E: J Proc Mech Eng, vol. 235, no. 2, 2020.
- [25] M. Ramanuja G. G. Krishna, H. K. Sree, and V. N. Radhika, "Free convection in a vertical slit microchannel with super-hydrophobic slip and temperature jump conditions", Int. J. Heat Tech, vol. 38, no. 3, pp. 738-744, 2020.
- [26] S. Hatte and R. Pitchumani, "Analysis of convection heat transfer on multiscale rough super-hydrophobic and liquid infused surfaces", pp. 1-29. <https://www.sciencedirect.com/science/article/am/pii/S13858947210184>
- [27] A O Ajibade and A U Umar, Effects of viscous dissipation on a steady mixed convection Couette flow of heat generating/absorbing fluid, Science Forum (Journal of Pure and Applied Sciences), vol 21, pp. 67-76
- [28] O. D. Makinde, "Aziz A. Boundary layer flow of a nanofluid past a stretching sheet with convective boundary condition", Int J Thermal Sci vol. 50, pp. 1326-32, 2011.

Nomenclature

B_0 = Constant magnetic flux density [kg/s².m²]
 G = Gravitational acceleration [m/s²]
 h = Width of the channel [m]
 $C_p C_v$ = Specific heats at constant pressure and constant volume [Jkg⁻¹K⁻¹]
 λ = Dimensionless slip length parameter
 γ = Dimensionless temperature jump parameter
 M = Magnetic field
 Br = Brinkman number
 K = Darcy number
 Nu = Dimensionless heat transfer rate
 T = Dimensionless temperature of the fluid [K]
 T_0 = Reference temperature [K]
 u = Dimensionless velocity of the fluid [ms⁻¹]
 y = Dimensionless distance between plates
 U_0 = Reference velocity [ms⁻¹]

Greek letters

β = Thermal expansion coefficient [K⁻¹]
 $\beta_i \beta_v$ = Dimensionless variables
 μ = Variable fluid viscosity [kgm⁻¹s⁻¹]
 k = Thermal conductivity [m.kg/s³.K]
 α = Thermal diffusivity [m²s⁻¹]
 γ_s = Ratios of specific heats ($C_p C_v$)
 σ = Electrical conductivity of the fluid [s³m²/kg]
 ρ = Density of the fluid [kgm⁻³]
 ν = Fluid kinematic viscosity [m²s⁻¹]

Appendix

$$C_1 = \frac{1}{1 + \gamma}, C_2 = \frac{-1}{1 + \gamma}, C_7 = \frac{b_5 \gamma}{1 + \gamma},$$

$$V_3 = \gamma C_7 - b_5, D_1 = \frac{\lambda D_{11} - D_{10} - D_2 b_2}{a_1},$$

$$F_2 = \frac{F_{14}}{F_{13}}, F_3 = \frac{b_1}{12R^2}, F_4 = \frac{b_2}{2R\sqrt{R}}, F_5 = \frac{-b_3}{2R\sqrt{R}}$$

$$F_6 = \frac{b_4}{12R^2}, F_7 = \frac{-b_5}{2R}, F_8 = \frac{C_7}{R}$$

$$b_1 = 1 - \lambda\sqrt{R}, b_2 = 1 + \lambda\sqrt{R}, b_3 = b_1 e^{-\sqrt{R}} - b_2 e^{\sqrt{R}}$$

$$b_4 = -b_1 - \lambda e^{\sqrt{R}}, b_5 = e^{\sqrt{R}} - b_1,$$

$$R = M^2 + \frac{1}{K}$$

